

K-

Corrosion Characteristics of K-Claddings

150

가 . 가 (K-
) K-
 가 , 360
 , 가 loop 400
 가 , K-
 Zry-4 A ,
 K6 K3 . K-
 , 가 가 .

Abstract

The Improvement of the corrosion resistance of nuclear fuel claddings is the critical issue for the successful development of the high burn-up fuel. KAERI have developed the K-claddings having a superior corrosion resistance by controlling the alloying element addition and optimizing the manufacturing process. The comparative evaluation of the corrosion resistance for K-claddings and the foreign claddings was performed and the effect of the heat treatment on the corrosion behavior of K-claddings was also examined. Corrosion tests were carried out in the conditions of 360 pure water, PWR-simulating loop and 400 steam, From the results of the corrosion tests, it was found that the corrosion resistance of K-claddings is superior to those of Zry4 and A claddings and K6 showed a better corrosion resistance than K3. The corrosion behavior of K-cladding was strongly influenced by the final annealing rather than the intermediate annealing, and the corrosion resistance increased with decreasing the final annealing temperature.

1.

가 , Nb 가
 가
 K- 가 ,
 1,2) Nb 가
 Nb 가
 3,4) K- 가 ,

2.

K- 가 K- Zr-1.5wt.%Nb-0.4wt.%Sn-(Fe,Cu)
 K3 Zr-1.1wt.%Sn-(Cu) K6
 Zr-1.0wt.%Nb-1.0wt.%Sn-0.1wt.%Fe A Zr-
 1.3wt.%Sn-0.2 wt.%Fe-0.1 wt.%Cr Zircaloy-4
 K , forging
 1 pilgering
 50.8mm TREX , 580 620
 TREX 3 pilgering
 9.5mm tube
 40mm , 5% HF, 45% HNO₃, 50%
 H₂O 360 , 18.5MPa
 가 loop 400 , 10.5MPa
 가 가
 가 .

10% HClO₃, 90% C₂H₅OH (TEM) , TEM
 twin-jet polishing X-

3.

Fig. 1 Fig. 2 K3 K6
 Zr (stress-relieved), (partially recrystallized) (fully recrystallized)

가 가 , 가 가
 가 K3 K6
 가 가

K3 K6 가
 Fig. 3 360 K3 Zry4 A

360 K6 Fig. 4
 K3 가 Zry4 A K6
 가 K3 , K6
 , Zry4
 , K

Fig. 5 PWR K3
 K3 PWR Zry4 A
 , 360

가 Fig. 6 PWR
 K6 , Zry4 A

Fig. 7 400 steam K3
 400 360 가 가
 가 , 470

K6 Fig. 8 400
 K6 400

가 가 470

Fig. 9 K3 K6 가 가 K

, Fig. 10 K3 K6 가 가

Fig. 11 K3 K6 K6 XRD K

가 가 가

Zr

5)

6) Zr

가

가

6)

K6

K3

K3

K6

Zry4

A

4.

(1) K-

가 , K-

Zry-4 A

K6

K3

(2) K-

가 가

- 1) H. Anada, B. H. Herb, K. Nomoto, S. Hagi, R. A. Graham and T. Kuroda, ASTM STP 1295 (1996) 74.
- 2) H. Anada, K. Nomoto and Y. Shida, ASTM STP 1245 (1994) 307.
- 3) G. P. Sabol, G. R. Kilp, M. G. Balfour and E. Roberts, ASTM STP 1023 (1989) 227.
- 4) J. -P. Mardon, D. Charquet and J. Senevat, ASTM STP 1354 (2000) 505.
- 5) P. Barberis and A. Frichet, J. Nucl. Mater. 273, 182 (1999).
- 6) J. Godlewski, Zirconium in the Nuclear Industry, ASTM STP 1245, 663 (1993).

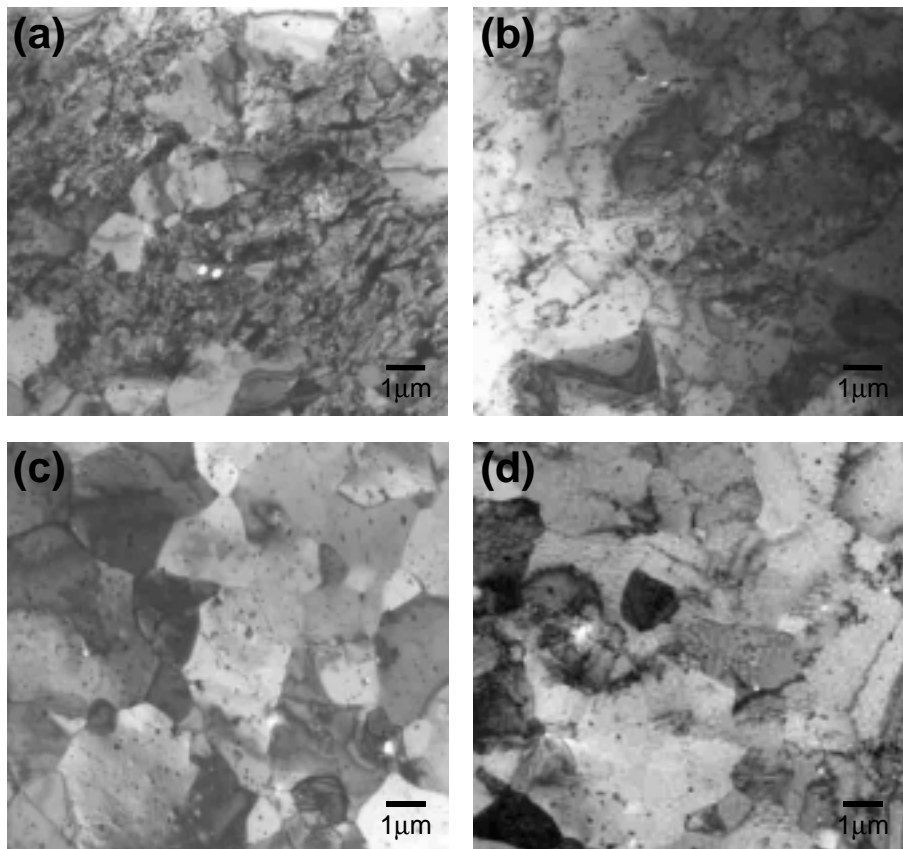


Fig. 1. Transmission electron micrographs of K3 claddings which are intermediate-annealed at 570°C and final-annealed at (a) 470°C, (b) 510°C and (c) 570°C, and (d) intermediate-annealed at 620°C and final-annealed at 510°C.

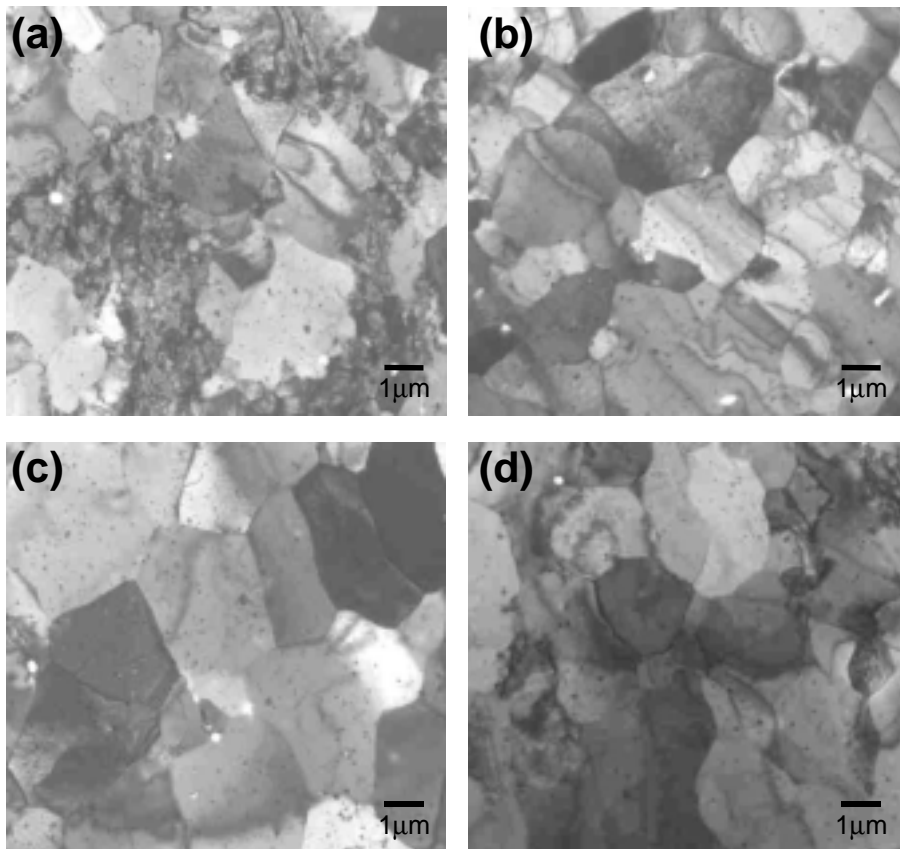


Fig. 2. Transmission electron micrographs of K6 claddings which are intermediate-annealed at 570°C and final-annealed at (a) 470°C, (b) 510°C and (c) 570°C, and (d) intermediate-annealed at 620°C and final-annealed at 510°C.

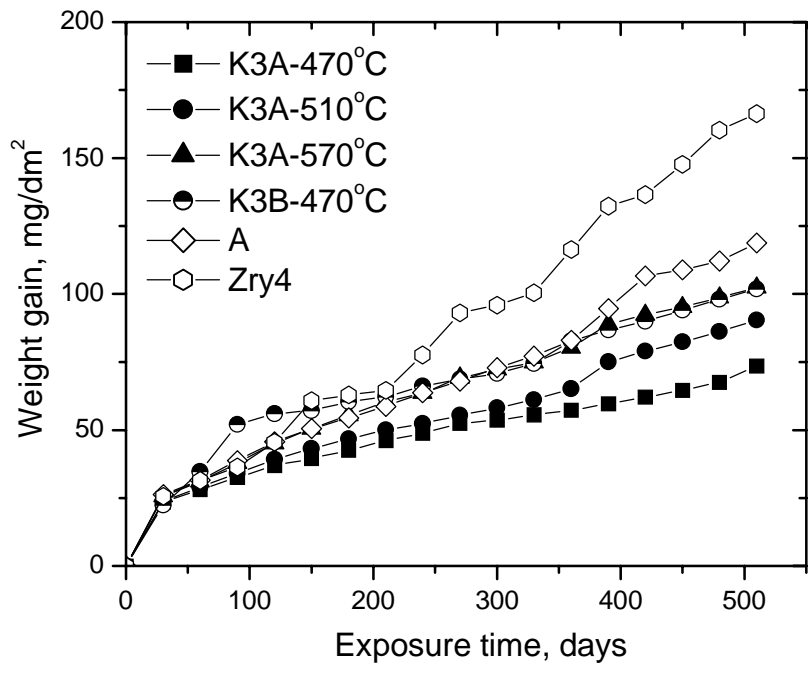


Fig. 3. Corrosion behavior of K3 claddings in 360°C pure water.

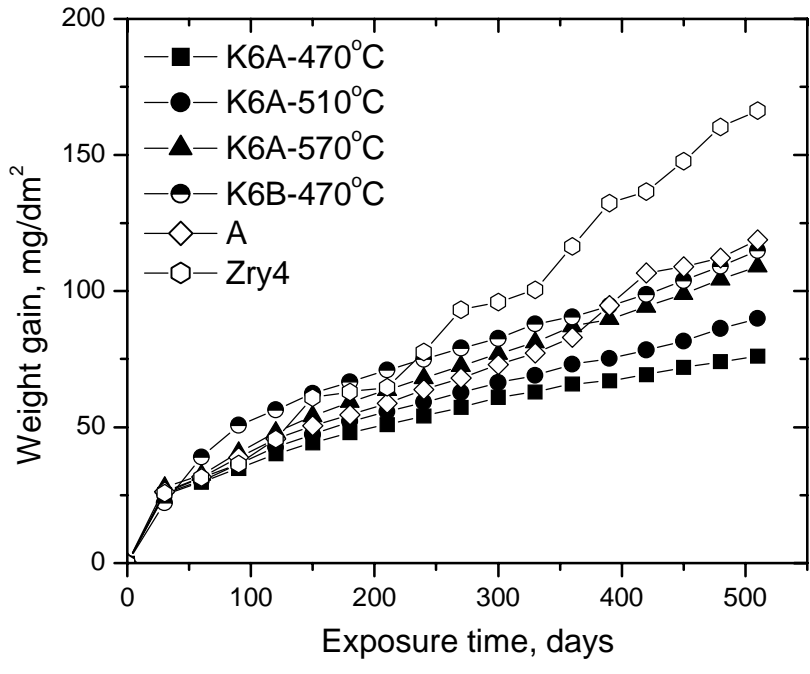


Fig. 4. Corrosion behavior of K6 claddings in 360°C pure water.

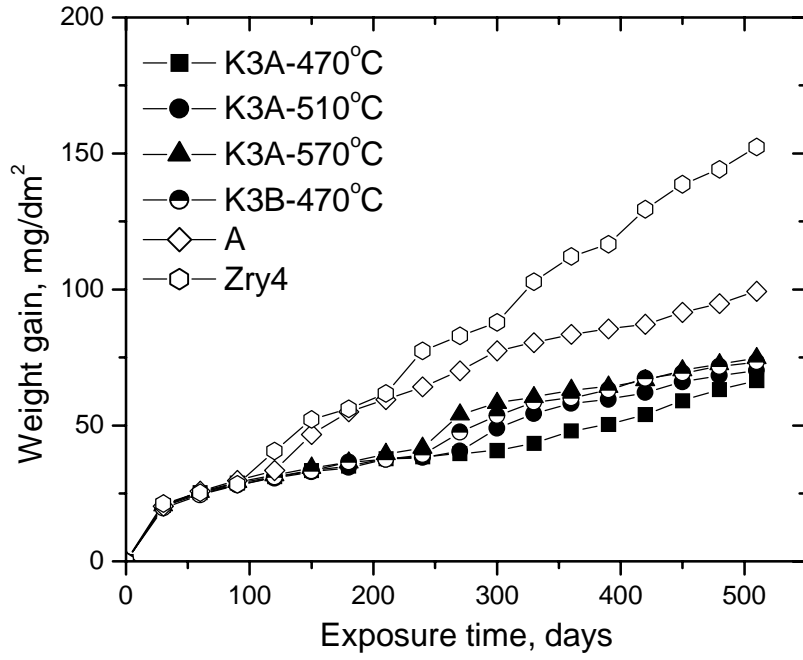


Fig. 5. Corrosion behavior of K3 claddings in PWR-simulating loop.

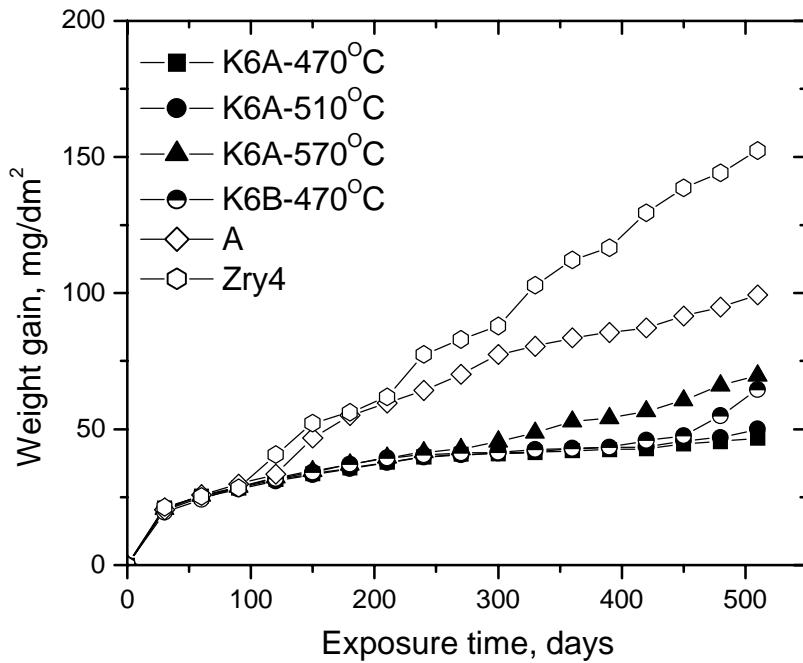


Fig. 6. Corrosion behavior of K6 claddings in PWR-simulating loop.

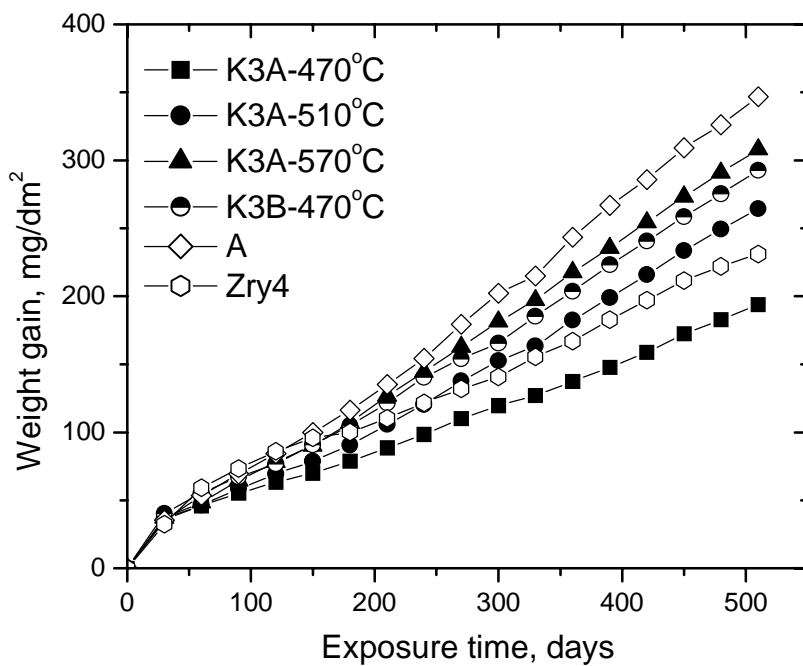


Fig. 7. Corrosion behavior of K3 claddings in 400°C steam.

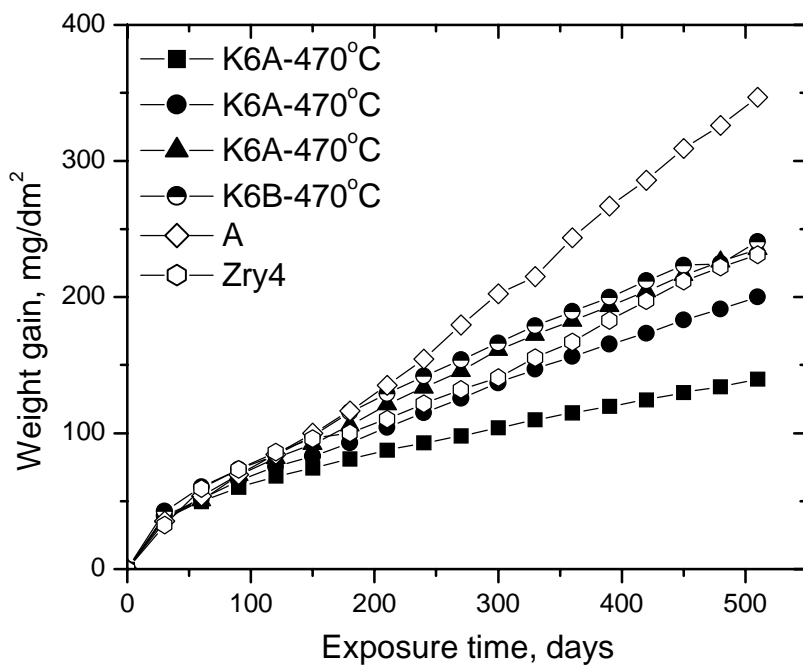


Fig. 8. Corrosion behavior of K6 claddings in 400°C steam.

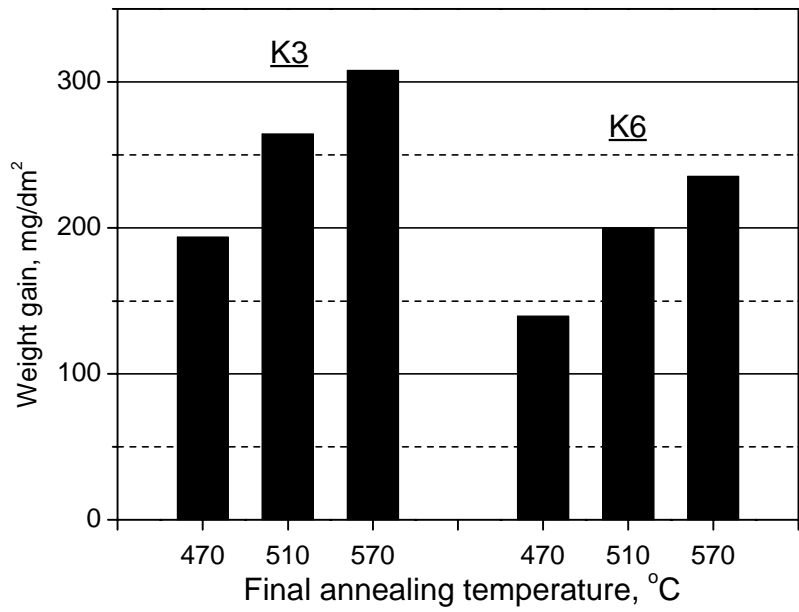


Fig. 9. Effect of final annealing temperature on the corrosion behavior of K3 and K6 claddings in 400°C steam.

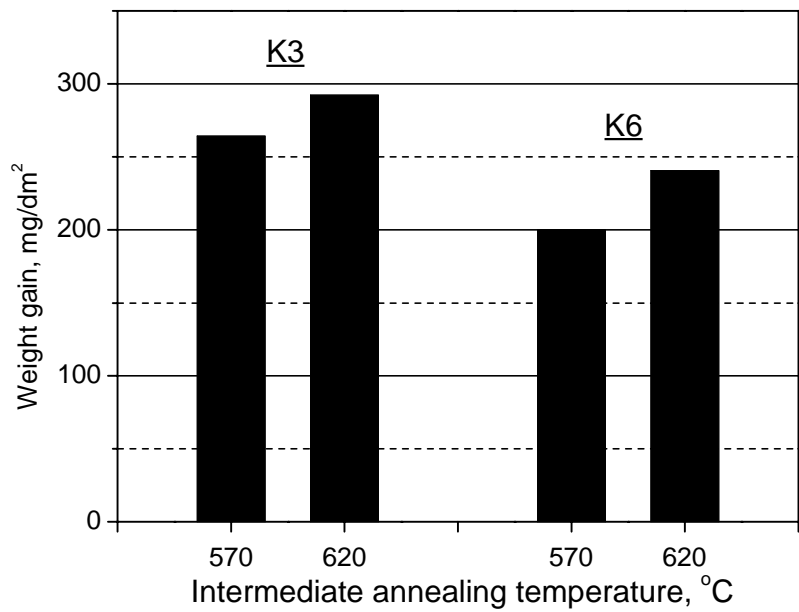


Fig. 10. Effect of intermediate annealing temperature on the corrosion behavior of K3 and K6 claddings in 400°C steam.

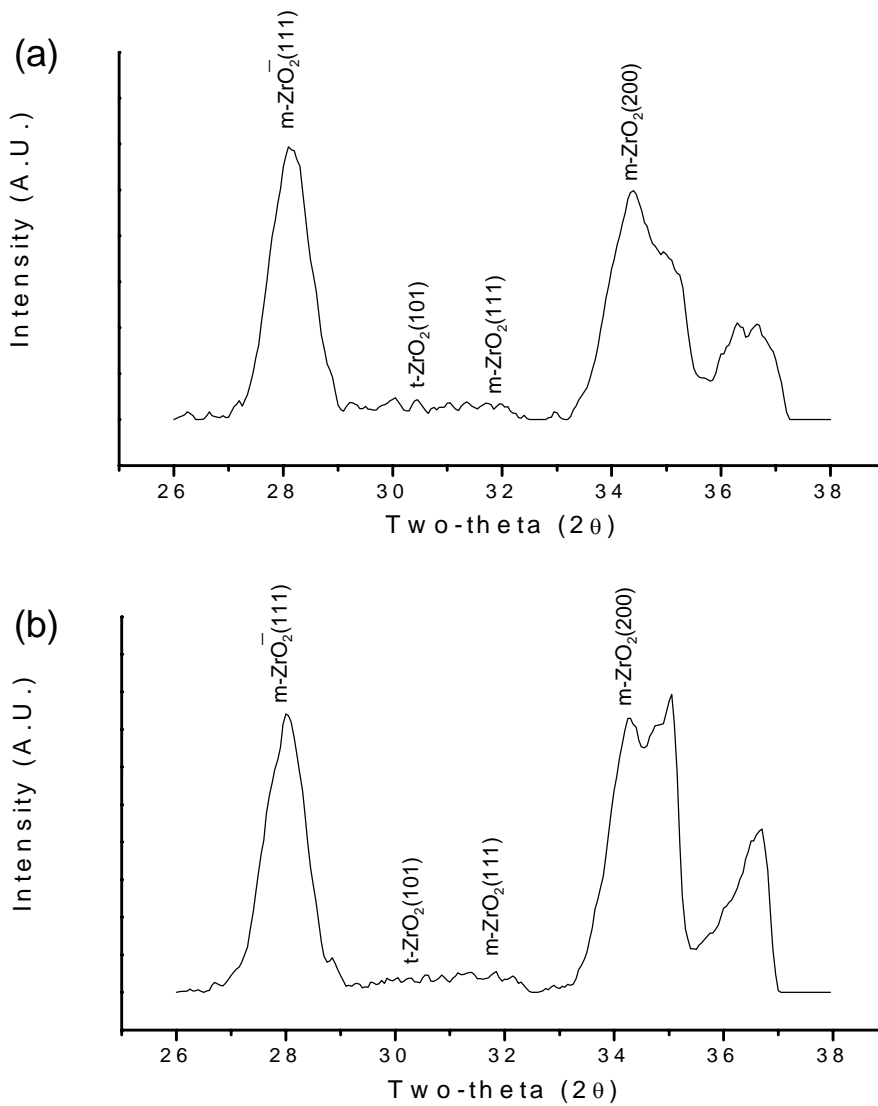


Fig. 11. X-ray diffraction results on the oxides formed on (a) K3 and (b) K6 claddings corroded to a weight gain of about $30\text{mg}/\text{dm}^2$ in PWR-simulating loop.